Membrane-bound serine protease matriptase-2 (Tmprss6) is an essential regulator of iron homeostasis

Alicia R. Folgueras,[1] Fernando Martín de Lara,[1] Alberto M. Pendás,[1] Cecilia Garabaya,[1] Francisco Rodríguez,[1] Aurora Astudillo,[2] Teresa Bernal,[3] Rubén Cabanillas,[4] Carlos López-Otín,[1] and Gloria Velasco[1]

[1]Departamento de Bioquímica y Biología Molecular, Facultad de Medicina, Instituto Universitario de Oncología, Universidad de Oviedo, Oviedo; and Servicios de [2]Anatomía Patológica, [3]Hematología, and [4]Otorrinolaringología, Hospital Universitario Central de Asturias, Oviedo, Spain

Proteolytic events at the cell surface are essential in the regulation of signal transduction pathways. During the past years, the family of type II transmembrane serine proteases (TTSPs) has acquired an increasing relevance because of their privileged localization at the cell surface, although our current understanding of the biologic function of most TTSPs is limited. Here we show that matriptase-2 (*Tmprss6*), a recently described member of the TTSP family, is an essential regulator of iron homeostasis. Thus, *Tmprss6*$^{-/-}$ mice display an overt phenotype of alopecia and a severe iron deficiency anemia. These hematologic alterations found in *Tmprss6*$^{-/-}$ mice are accompanied by a marked up-regulation of hepcidin, a negative regulator of iron export into plasma. Likewise, *Tmprss6*$^{-/-}$ mice have reduced ferroportin expression in the basolateral membrane of enterocytes and accumulate iron in these cells. Iron-dextran therapy rescues both alopecia and hematologic alterations of *Tmprss6*$^{-/-}$ mice, providing causal evidence that the anemic phenotype of these mutant mice results from the blockade of intestinal iron export into plasma after dietary absorption. On the basis of these findings, we conclude that matriptase-2 activity represents a novel and relevant step in hepcidin regulation and iron homeostasis. (Blood. 2008;112:2539-2545)

Introduction

Pericellular proteolysis is an essential event that determines the relations between the cell and its microenvironment. This crucial process in the development and maintenance of multicellular organisms requires the remodeling of extracellular matrix components as well as the posttranslational regulation of a wide range of cell-surface receptors, regulatory proteins, and adhesion molecules.[1] The increasing relevance of proteolytic processes localized at the cell surface has attracted notable attention on membrane-associated proteolytic systems, including the family of type II transmembrane serine proteases (TTSPs).[2,3] The TTSP family is composed of more than 20 different members that share a number of structural features: a single-pass transmembrane domain located near the short cytoplasmic amino-terminal tail, a central region containing different protein-interacting domains, and a carboxy-terminal catalytic region with the structural characteristics of serine proteases. The large variability of the central modular region together with the diverse expression patterns of TTSP family members suggest that these enzymes may play different physiologic and pathologic roles, although only a few of these functions have been identified so far. Thus, enteropeptidase is mainly expressed in the duodenum and plays an essential role in food digestion as activator of pancreatic trypsinogen to trypsin.[4] Hepsin, is mainly expressed in liver, but it is highly up-regulated in prostate cancer.[5,6] Matriptase/MT-SP1 is a widely studied member of the TTSP family because of its relevance in diverse processes, including cancer progression.[7,8] Mutant mice deficient in matriptase die shortly after birth because of aberrant skin development that compromises epidermal barrier function and causes mice dehydration.[9] Corin is a TTSP family member mainly expressed in the heart and involved in the activation of proatrial natriuretic peptide, a cardiac hormone essential for the regulation of blood pressure.[10] TMPRSS2 and TMPRSS4 are up-regulated or structurally altered in prostate cancer.[11,12] Other members of this protease family whose physiologic and pathologic roles still remain unclear are spinesin/TMPRSS5,[13] MSPL (mosaic serine protease large form),[14] matriptase-3,[15] polyserase-1,[16] as well as the different components of the HAT (human airway trypsin-like protease)/DESC (differentially expressed in squamous cell carcinoma) subfamily.[17,18]

Matriptase-2 (TMPRSS6) is another TTSP family member of unknown function, but whose study has achieved particular interest because of its structural and enzymatic similarities with matriptase and to its putative role as a tumor suppressor enzyme in human breast cancer.[19-21] This enzyme was first identified and cloned in our laboratory[19] as part of our ongoing studies aimed at characterizing the human degradome, which is defined as the complete set of proteases produced by human cells.[22,23] Matriptase-2 expression is mainly circumscribed to liver in both human and mouse, suggesting tissue-specific functions for this enzyme.[19,24] Nevertheless, minor matriptase-2 expression has also been detected in kidney, uterus, and the nasal cavity.[24] Matriptase-2 shares the structural organization of TTSPs, including the short cytoplasmic domain, a type II transmembrane sequence, a stem region with 2 CUB (*c*omplement factor C1s/C1r, *u*rchin embryonic growth factor, *b*one morphogenetic protein) domains and 3 LDLR (*low-d*ensity

*li*poprotein *r*eceptor) tandem repeats, and the carboxy-terminal serine protease domain.[19,24] In addition, matriptase-2 contains a SEA (*se*a urchin sperm protein, *e*nteropeptidase, *a*grin) domain that conserves a potential cleavage motif sequence that may release the enzyme from the cell surface, as reported for other TTSPs.[20] Matriptase-2 can degrade in vitro extracellular matrix components such as fibronectin, fibrinogen, and type I collagen and to activate single-chain uPA although with low efficiency compared with matriptase.[19] However, at present, little information is available about the in vivo functional relevance of matriptase-2 in both physiologic and pathologic processes. To further characterize the in vivo role of this type II transmembrane serine protease, we have generated mutant mice deficient in matriptase-2. In this work, and after a series of phenotypic and molecular analysis of *Tmprss6*^{−/−} mice, we provide evidence that matriptase-2 is an essential regulator of iron homeostasis.

Methods

Tmprss6 gene targeting

A 3′-*Hprt* chromosomal engineering targeting vector was used to generate *Tmprss6*^{−/−} mice following an insertional targeting strategy.[25] A 7068-bp homology region, containing exons 3 to 6, was amplified by polymerase chain reaction (PCR) from a murine genomic 129S7-derived PAC clone by using Long-Expand High Fidelity PCR mix (Roche Applied Science, Indianapolis, IN), and it was cloned into the *Asc*I site of the 3′-*Hprt* vector (a kind gift of Dr A. Bradley, Wellcome Trust Sanger Institute, Hinxton, United Kingdom). The targeting vector was digested with *Eco*RI to remove an internal *Eco*RI fragment in the homology region and to create a "gap" that will be repaired during the targeting event. The targeting vector was linearized by digestion with *Eco*RI and electroporated into HM-1 embryonic stem cells. Resistant clones were selected with puromycin by using standard protocols. Homologous recombination was confirmed in the screened clones by Southern blot hybridization with the gap region which was used as a probe, after *Nde*I digestion. During the targeting event the gap is repaired and, as a consequence of the duplicated region generated, a novel 18-kb fragment is detected by the gap probe in addition to the 9-kb wild-type fragment. The heterozygous stem cells identified were aggregated to CD1 morulas and transferred into uteri of pseudopregnant females to generate chimeras. Chimeric males were mated with C57BL/6J females. A new strategy of genotyping was used to screen the offspring by using Southern blotting analysis of tail genomic DNA digested with *Ssp*I and hybridized with a 3′-external probe amplified from a genomic PAC. This probe was a 593-bp fragment amplified with primers 5′-GTCTCAGGTTCCCTGAGCCTG-3′ and 5′-GTGCCAAA-CACTCAGGG ATGC-3′.

Northern blot analysis

Total RNA was isolated from frozen liver samples obtained from wild-type and mutant adult mice by using a commercial kit (RNeasy Mini Kit; Qiagen, Valencia, CA). A total 10 μg denatured RNA from liver was separated by electrophoresis on agarose gels and transferred to Hybond N+ (GE Healthcare, Little Chalfont, United Kingdom). Blots were hybridized with random primed ^{32}P-labeled cDNA probes for mouse *Tmprss6* and hepcidin. The cDNA probe for hepcidin was obtained by reverse transcription-PCR (RT-PCR) using 1 μg total RNA from mouse liver and oligodT as primer, according to the manufacturer's instructions (Invitrogen, Carlsbad, CA). After RT, 2 μL of the mixture were used for PCR with the following murine hepcidin-specific oligonucleotides: mHepcidinFw, 5′-CAGCAGAA-CAGAAGGCATGA; and mHepcidinRv, 5′-AGATGCAGATGGGGA AGTTG. The specific probe used to detect *Tmprss6* was prepared from the murine *Tmprss6* cDNA plasmid by digestion with *Bam*HI. Blots were rehybridized with a beta-actin (*Actb*) cDNA probe as an indicator of RNA loading.

Transcriptional profiling and real-time quantitative PCR

Total RNA was isolated as described before. Double-stranded cDNA was synthesized using the SuperScript cDNA synthesis kit (Invitrogen). In vitro transcription was carried out with the Bioarray high yield RNA transcript labeling kit (Enzo Diagnostics, New York, NY). The biotin-labeled cRNA was purified, fragmented, and hybridized to GeneChip Mouse 430 2.0 Array (Affymetrix, Santa Clara, CA). All microarray data have been deposited in Gene Expression Omnibus (GEO) of NCBI through accession number GSE11632.[25] Real-time quantification of hepcidin transcript levels was performed by using Applied Biosystems Taqman gene expression assays in an ABI7000 Sequence detection system (Applied Biosystems, Foster City, CA) following the manufacturer's instructions. Hepcidin transcript abundance was calculated in triplicated relative to the expression of the stable housekeeping gene *Actb*. The average relative expression of hepcidin in wild-type mice was assigned an arbitrary value of 100 in each experiment.

Blood analysis and iron-dextran treatment

Mouse experimentation was done according to the guidelines of the University of Oviedo (Oviedo, Spain). Whole blood was collected retro-orbitally into heparinized-coated tubes. Plasma iron and unsaturated iron binding capacity (UIBC) were determined using a colorimetric method (Biolabo, Maizy, France). The total iron binding capacity (TIBC) was calculated as the sum of plasma iron and UIBC, and the percentage of transferrin saturation used the formula plasma iron/TIBC × 100. Peripheral blood smears were stained with Wright-Giemsa stain (Fisher Scientific, Pittsburgh, PA) for morphologic examination. Where indicated, 5 mg (8-week-old) or 2 mg (10-day-old) iron-dextran (Sigma-Aldrich, St Louis, MO) was injected subcutaneously weekly to knock-out mice.

Tissue iron staining and immunohistochemistry

Duodenal samples were fixed in 4% formaldehyde and embedded in paraffin. Deparaffined tissue sections were stained with Perls Prussian blue stain for nonheme iron, after nuclear red counterstaining by using standard procedures. To perform immunohistochemistry analysis, deparaffined and rehydrated sections were rinsed in PBS (pH 7.5). Sections were incubated overnight at 4°C with a rabbit polyclonal antibody anti–mouse ferroportin (LifeSpan Biosciences, Seattle WA), diluted 1:100. Then sections were incubated with an anti–rabbit EnVision system–labeled polymer-HRP (Dako North America, Carpinteria, CA) for 30 minutes, washed, and visualized with diaminobenzidine. Sections were counterstained with Mayer hematoxylin, dehydrated, and mounted in Entellan. Sections were examined using a Nikon Eclipse E400 microscope, and images were acquired with a Nikon DS-Si1 camera and Nikon NIS-Elements F2.20 software (Nikon, Melville, NY).

Statistical analysis

The mean values and the corresponding standard error of the means (SEMs) were calculated. Differences between mean values were analyzed by 2-tailed Student *t* test. A value of *P* less than .05 was considered significant. Statistically significant differences are shown with asterisks.

Results

Generation of mice deficient in matriptase-2

To analyze the in vivo role of matriptase-2, we designed an insertion vector for gene targeting, to provide a high targeting frequency[26] (Figure 1A). According to this strategy, after electroporation into HM-1 embryonic stem cells (129/Ola background), the linearized and gapped vector would integrate into the target locus generating a duplication of the entire region of homology, including the repaired gap sequence (Figure 1B). By following this procedure, we finally identified several correctly targeted clones that were used to generate chimeras and finally heterozygous mice.

Figure 1. Gene targeted disruption of the *Tmprss6* gene. (A) Partial genomic structure of the murine *Tmprss6* gene (top). Exon coding sequences are indicated as black bars. The targeting vector duplicates exons III to VI (bottom). E indicates *Eco*RI; S, *Ssp*I; N, *Nde*I; 3′*Hprt*, 3′-half *Hprt* minigene; *Puro*, puromycin resistance gene; *Ag*, *K14 Agouti* minigene. (B) Predicted structure of the targeted allele. (C) Southern blot analysis of DNA from *Tmprss6*$^{+/+}$, *Tmprss6*$^{+/−}$, and *Tmprss6*$^{−/−}$ mice digested with *Ssp*I. Hybridization with the 3′-external probe detects the expected 33-kb and 9-kb bands corresponding to wild-type and mutant alleles, respectively. (D) Northern blot analysis of liver tissues obtained from wild-type and *Tmprss6*$^{−/−}$ mice showing the absence of full-length *Tmprss6* mRNA expression in mutant mice.
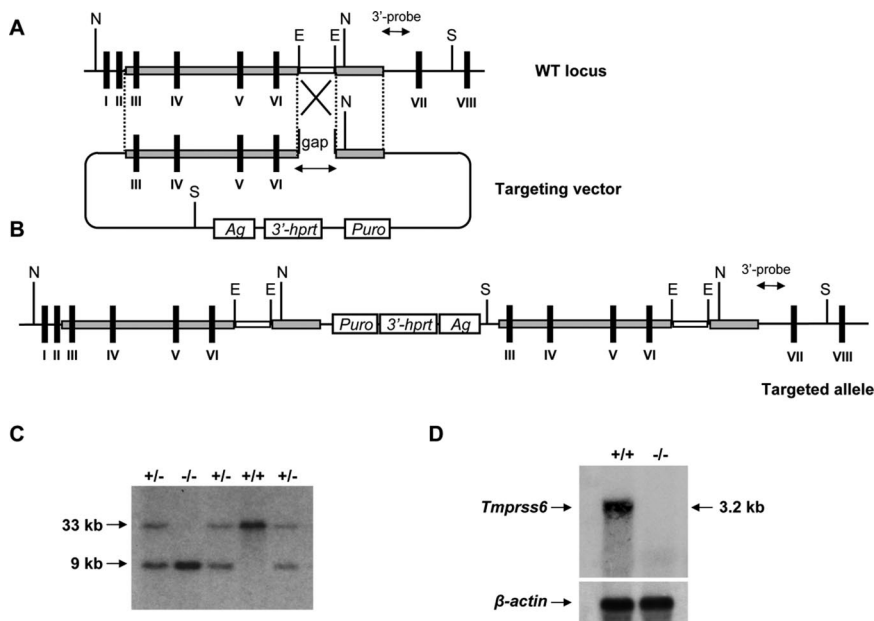
After intercrossing heterozygous mice from the F1 generation, we obtained *Tmprss6*$^{+/+}$, *Tmprss6*$^{+/−}$, and *Tmprss6*$^{−/−}$ mice in the expected Mendelian ratios (Figure 1C). Northern blot analysis of total RNA from liver of wild-type and knock-out animals confirmed the complete absence of *Tmprss6* transcript in *Tmprss6*$^{−/−}$ mice (Figure 1D). *Tmprss6*$^{−/−}$ mice exhibited slight signs of growth retardation that were more pronounced in female mice. Thus, we observed significant differences between the body weight of 4-week-old control and mutant female mice (control, 12.0 ± 0.4 g, n = 26, vs knockout, 10.2 ± 0.5 g, n = 15; $P < .05$). Likewise, we observed a marked retardation in ovarian maturation in adult *Tmprss6*$^{−/−}$ females that could be linked to the infertility observed in these mutant females.

Tmprss6$^{−/−}$ mice exhibit a cyclic hair loss phenotype

Mice deficient in *Tmprss6* display an overt phenotype of alopecia. Knockout pups started to show hair loss on the back at approxi-

mately 2 weeks of age, although the head of these mutant mice did not show any evidence of hair loss. By 4 weeks of age, *Tmprss6*$^{−/−}$ mice displayed a completely nude phenotype in the dorsal and ventral regions of the thorax and abdomen (Figure 2A). This alopecia condition lasted for approximately 10 days, and then new hair growth was initiated, as shown by the change in back skin color followed by a complete recovery of the hair. A few days later, a progressive hair loss began again, and a phenotype of diffuse alopecia in the dorsal region was definitively maintained during adult life. Histologic analysis showed that skin from 4-week-old mice had a reduced number of pillar units and the hair follicles were disorganized, dystrophic, and hypoplastic, showing a thinner outer root sheath at the isthmus and inferior segment level. Likewise, mutant mice displayed a pronounced infundibular ectasia with hyperkeratosis (Figure 2B). In adult *Tmprss6*$^{−/−}$ mice, the reduced number of pillar units as well as the hypoplastic phenotype were also observed in
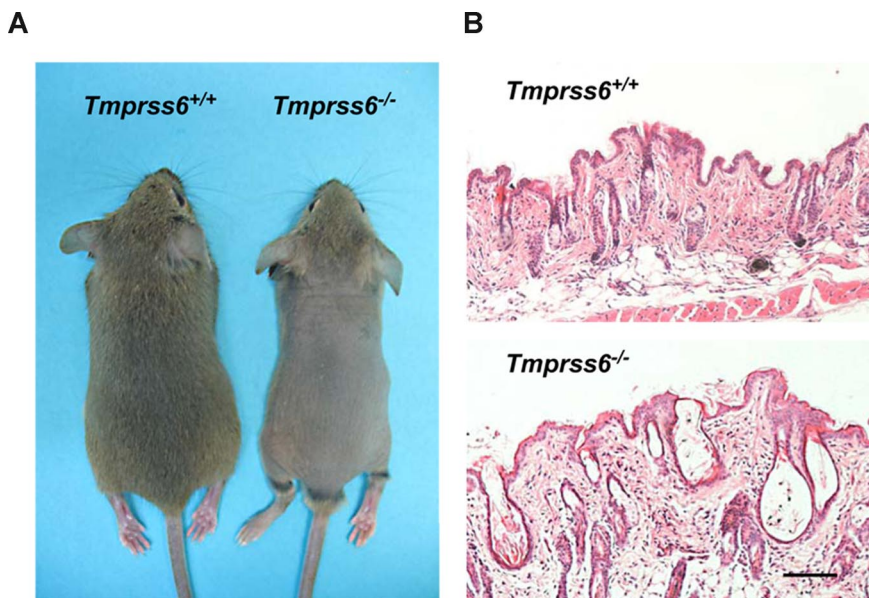

Figure 2. Alopecia phenotype in *Tmprss6*$^{−/−}$ mice. (A) Representative photographs of 4-week-old *Tmprss6*$^{+/+}$ and *Tmprss6*$^{−/−}$ littermate mice. (B) Skin sections from 4-week-old wild-type and *Tmprss6*$^{−/−}$ mice showing dystrophic hair follicles and hyperkeratosis in *Tmprss6*-null tissue, compared with the wild-type. Bar represents 100 μm; magnification, 20×/0.40 NA.

Table 1. Reduced plasma iron and transferrin saturation in *Tmprss6*$^{-/-}$ mice

	Plasma iron, µg/dL	UIBC, µg/dL	Tf saturation, %
Tmprss6$^{+/+}$	113.3 ± 6.6	237.5 ± 41.5	34.1 ± 3.5
Tmprss6$^{-/-}$	47.9 ± 5.8*	375.2 ± 14.6†	11.3 ± 1.3*

Plasma iron content, unsaturated iron binding capacity (UIBC), and transferrin (Tf) saturation were determined in 6-week-old wild-type and *Tmprss6*$^{-/-}$ mice. Data are shown as means plus or minus SEM.

*$P <$ .001, 6 mice per group.

†$P <$ .05, 6 mice per group.

the skin. However, the hyperkeratosis and ectasia almost disappeared (data not shown).

Hepcidin up-regulation causes severe anemia in *Tmprss6*$^{-/-}$ mice

The phenotypic features of hair loss present in *Tmprss6*$^{-/-}$ mice, together with the observation of an evident pallor phenotype in newborn mice and the occurrence of several signs of growth retardation and female infertility, prompted us to analyze a series of hematologic variables in blood samples of these mutant mice. Plasma analysis showed that *Tmprss6*$^{-/-}$ mice were anemic and displayed both a severe iron deficiency and reduced transferrin saturation (Table 1). Likewise, Wright-Giemsa–stained blood smears from *Tmprss6*$^{-/-}$ mice showed a severe hypochromia and a slight phenotype of anisocytosis and poikilocytosis in comparison to wild-type counterparts (Figure 3A,B). These morphologic observations were confirmed after the quantification of several red blood cell variables (Table 2). Considering this anemic phenotype observed in *Tmprss6*$^{-/-}$ mice and the restricted expression pattern of this protease, which is mainly circumscribed to the liver, we hypothesized that the absence of matriptase-2 (*Tmprss6*) in this essential organ for iron homeostasis might alter certain regulatory factors involved in iron metabolism, alterations which could in turn contribute to explain the observed phenotype. To evaluate this possibility, we used oligonucleotide-based microarrays to analyze transcriptional changes in liver from *Tmprss6*$^{-/-}$ mice. Of 45 000 gene sequences present in the array, a total of 471 (1.05%) showed a higher than 2.5-fold decrease in expression levels in liver from *Tmprss6*$^{-/-}$ compared with control mice, whereas 221 genes (0.49%) were up-regulated more than 2-fold (Table S1, available on the *Blood* website; see the Supplemental Materials link at the top of the online article). Analysis of these results showed that hepcidin, the principal hormonal regulator of systemic iron homeostasis, was clearly up-regulated in *Tmprss6*$^{-/-}$ mice compared with wild-type animals. Northern blot analysis and quantitative PCR of liver RNAs from different *Tmprss6*$^{-/-}$ mice confirmed that hepcidin was significantly up-regulated (2.5-fold increase) in mice deficient in this serine protease (Figure 3C,D). Additional studies showed that this hepcidin up-regulation was already present in *Tmprss6*$^{-/-}$ mice since birth. Thus, *Tmprss6*$^{-/-}$ newborn mice showed a 4.8-fold increase in expression levels of liver hepcidin in comparison to control mice (knockout, 485.7 ± 84.0, vs control, 100.0 ± 25.1; $P <$ .01; n = 5 mice per genotype).

Because hepcidin is a negative regulator of iron export into plasma, we next explored the putative occurrence of iron deposits in the duodenum to evaluate whether the anemic phenotype of *Tmprss6*$^{-/-}$ mice could be due to a defective iron release into the circulation after diet absorption. Interestingly, Perls staining showed notable cellular iron retention in duodenal enterocytes of *Tmprss6*$^{-/-}$ mice (Figure 3E,F). Then, and considering that hepcidin blocks iron release through the down-regulation of ferroportin (the only known cellular iron exporter), we examined by immunohistochemistry the expression of this protein in the duodenum of wild-type

and *Tmprss6*$^{-/-}$ mice. As shown in Figure 3G, a marked positive staining was observed in the basolateral membrane of duodenal enterocytes of wild-type mice. By contrast, ferroportin expression
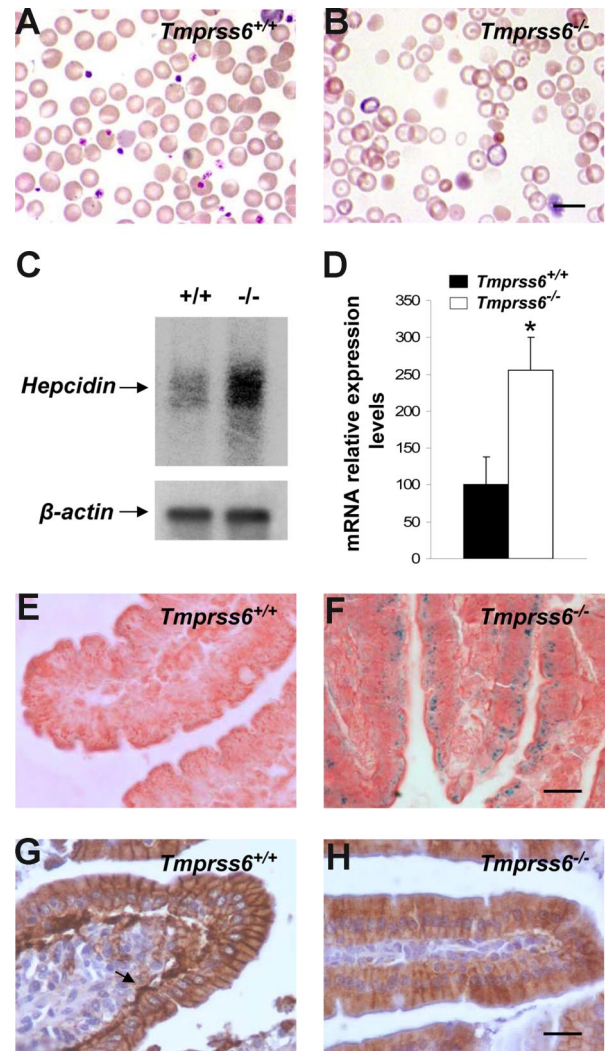

Figure 3. Hepcidin up-regulation reduces ferroportin expression and causes an anemic phenotype in *Tmprss6*$^{-/-}$ mice. Wright-Giemsa–stained blood smears from *Tmprss6*$^{+/+}$ (A) and *Tmprss6*$^{-/-}$ (B) littermate mice. The figure shows the severe hypochromia found in mutant erythrocytes in comparison to wild-type ones. (C) Representative Northern blot analysis of liver tissues from wild-type and *Tmprss6*$^{-/-}$ mice showing the increased hepcidin mRNA expression in mutant mice. (D) TaqMan real-time PCR analysis of hepcidin expression in liver samples from 7-week-old *Tmprss6*$^{+/+}$ and *Tmprss6*$^{-/-}$ mice. mRNA levels on the y-axis are expressed relative to β-actin levels. The average relative expression of hepcidin in wild-type mice was assigned an arbitrary value of 100. Values are means (± SEM). *$P <$ .05; n = 5 mice per group. Perls Prussian blue stain for iron in sections of duodenal villi of 5-week-old *Tmprss6*$^{+/+}$ (E) and *Tmprss6*$^{-/-}$ (F) mice shows iron accumulation in *Tmprss6*-null enterocytes. Representative immunostaining of ferroportin in duodenal tissue from 5-week-old *Tmprss6*$^{+/+}$ (G) and *Tmprss6*$^{-/-}$ (H) mice. Arrow points to the basal expression of ferroportin in wild-type enterocytes, whereas positive basal staining is absent in *Tmprss6*-null cells. Bars represent 10 µm, magnification 100×/1.25 NA (A,B); bars 20 µm, magnification 60×/0.80 NA (E-H).

Table 2. Red blood cell parameters of *Tmprss6*$^{-/-}$ mice

	Hgb, g/dL	Hct, %	MCV, fL	MCH, pg	MCHC, g/dL
Tmprss6$^{+/+}$	16.4 ± 0.3	51.5 ± 1.1	49.8 ± 0.9	15.8 ± 0.2	31.8 ± 0.6
Tmprss6$^{-/-}$	12.0 ± 0.5*	44.3 ± 1.9†	37.5 ± 0.4*	10.2 ± 0.2*	27.1 ± 0.8‡

Hemoglobin (Hgb), hematocrit (Hct), mean cell volume (MCV), mean cell hemoglobin (MCH), and mean cell hemoglobin concentration (MCHC) were determined in 8-week-old wild-type (n = 5) and *Tmprss6*$^{-/-}$ (n = 4) mice. Data are shown as mean plus or minus SEM.

*$P < .001$.

†$P < .05$.

‡$P < .01$.

was almost absent in the basal membrane of *Tmprss6*$^{-/-}$ enterocytes (Figure 3H). Taken together, these results provide strong support to the hypothesis that the marked hepcidin up-regulation observed in *Tmprss6*$^{-/-}$ mice leads to the subsequent ferroportin removal of the enterocytes from these animals, impairing iron export into plasma and finally leading to iron deficiency anemia in *Tmprss6*$^{-/-}$ mice.

Iron therapy rescues alopecia and anemic phenotypes in *Tmprss6*$^{-/-}$ mice

The above-mentioned findings showing that iron deficiency anemia in *Tmprss6*$^{-/-}$ mice was probably due to an impaired iron export into plasma, prompted us to consider the possibility of rescuing this phenotype by directly releasing iron into the circulatory system. Thus, *Tmprss6*$^{-/-}$ adult mice received weekly an iron-dextran subcutaneous injection for a period of 4 weeks, and the occurrence of putative changes in their alopecia and hematologic phenotypes was examined. As can be seen in Figure 4A, this iron-based therapy led to a complete recovery of hair in treated knock-out mice (Figure 4A). Likewise, this iron therapy rescued the hematologic deficiencies observed in *Tmprss6*$^{-/-}$ mice. Thus, blood smear examination showed a marked reduction of hypochromic red cells in treated *Tmprss6*$^{-/-}$ mice (Figure 4B). Finally, we evaluated whether the initial hair loss phenotype observed in young knockout mice was also iron dependent. To this purpose we used a group of 10-day-old *Tmprss6*$^{-/-}$ pups, which received weekly an iron-dextran subcutaneous injection for a period of 3 weeks. Consistent with the above-mentioned findings in adult mice, this treatment completely prevented hair loss in all treated young animals (n = 4; data not shown).

Discussion

A tightly regulated iron homeostasis is essential for life maintenance in eukaryotic organisms. Both iron deficiency and iron overload cause severe disorders in humans.[27] Stable plasma concentrations and adequate levels of cellular iron are maintained through the strict control of a series of critical steps that regulate its absorption, transport, storage, and recycling. During the past years, the use of loss- and gain-of-function animal models together with genetic studies in patients with inherited iron homeostasis disorders have allowed the identification of key genes involved in iron metabolism.[28,29] Most of these genes are iron transporters specific of different cell types. However, our unexpected findings derived from the phenotype analysis of *Tmprss6*$^{-/-}$ mice show for the first time that the lack of a proteolytic enzyme has severe consequences on iron balance under normal conditions. Thus, after generation and phenotype analysis of these mutant mice we first observed that *Tmprss6* deficiency leads to severe iron deficiency anemia and hair loss. Further molecular analysis of tissues from the generated mutant mice showed that matriptase-2 is required for the maintenance of normal hepcidin expression levels as assessed by the finding that *Tmprss6*$^{-/-}$ mice showed significantly up-regulation in liver of the gene encoding this antimicrobial peptide. It is well established that hepcidin is a negative regulator of iron export, which is primarily secreted by hepatocytes and acts as a circulating hormone.[30] Mice deficient in hepcidin and patients with mutations in this gene display a severe iron overload disorder.[31,32] Conversely, transgenic mice overexpressing hepcidin in liver develop severe iron deficiency anemia.[33] Furthermore, it was recently shown that hepcidin controls iron levels through the binding to ferroportin, the
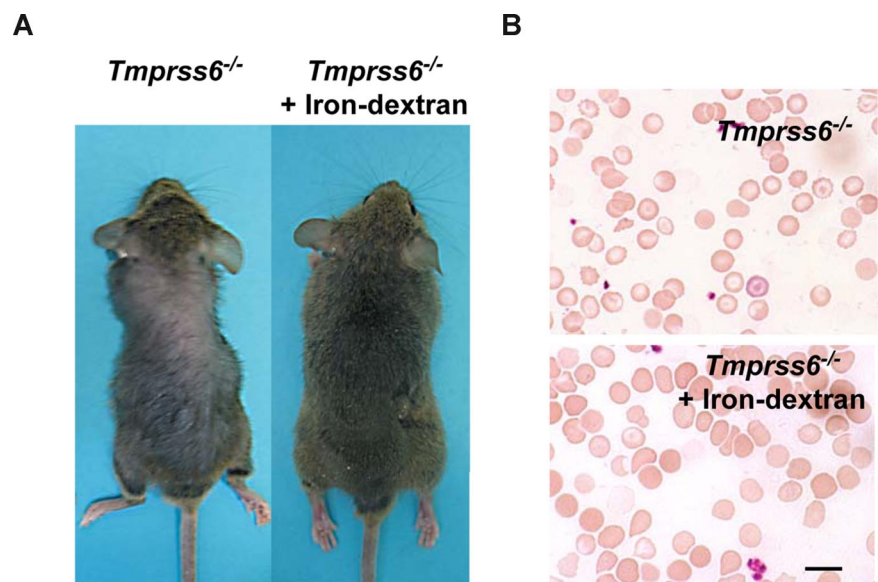

Figure 4. Iron-dextran therapy rescues the *Tmprss6*$^{-/-}$ phenotype. (A) Representative photograph of a 2-month-old *Tmprss6*$^{-/-}$ mice before (left) and after 1 month of iron-dextran treatment (right). (B) Wright-Giemsa–stained blood smears from untreated (top) and iron-dextran injected (bottom) *Tmprss6*$^{-/-}$ mice. Bar represents 10 μm; magnification, 100×/1.25 NA.

major iron exporter into the plasma. Thus, hepcidin binding results in ferroportin internalization from the cell surface with the subsequent degradation in lysosomes.[34] It is also remarkable that conditional disruption of the *ferroportin 1* gene causes iron deficiency anemia and iron accumulation in enterocytes.[35] Consistent with the marked up-regulation of hepcidin, mice deficient in matriptase-2 show both a dramatic decrease in ferroportin levels at the basal membrane of duodenal cells and a marked increase in iron deposits in these enterocytes. Furthermore, the rescue of the hematologic phenotype after iron treatment of these mutant mice reinforces the hypothesis that the anemic phenotype observed in *Tmprss6*^{−/−} mice results from the blockade of intestinal iron export into plasma after dietary absorption.

Upstream regulators responsible for the control of hepcidin expression have become the focus of attention in recent years because of their importance in the understanding of anemia and iron overload pathologies. According to our results, matriptase-2 is a novel candidate to act as in vivo regulator of hepcidin levels and function. Hepcidin is mainly regulated at the transcriptional level in response to a number of processes that affect iron balance, such as defective erythropoiesis, anemia, hypoxia, and inflammation.[36,37] Bone morphogenetic proteins (BMPs) are the main positive regulators of hepcidin transcription under normal conditions.[38] Binding of specific BMP ligands to BMP type I or type II receptors, located at the cell surface of hepatocytes, leads to an intracellular signaling cascade that results in phosphorylation of receptor Smads (Smad1, Smad5, and Smad8) that complex Smad4 to activate hepcidin transcription. Interestingly, it was recently described that hemojuvelin, a GPI-linked protein located at the cell surface of hepatocytes, acts as a BMP coreceptor promoting hepcidin transcription.[38] However, soluble hemojuvelin released from the cell surface was shown to be a competitive antagonist of membrane-bound hemojuvelin, leading to a decrease in hepcidin transcription.[39,40] In addition, it was reported that the in vitro shedding of BMP receptors reduces Smad signaling activation in primary human bone cells.[41] These results suggest that proteolytic activity at the cell surface of hepatocytes might be considered as an important step in hepcidin regulation and iron balance. Nevertheless, further studies will be necessary to elucidate whether matriptase-2 is the protease responsible for these proteolytic events presumably occurring at the pericellular space.

In conclusion, our results provide the first causal evidence that the absence of a protease has severe consequences on iron homeostasis under normal conditions. These findings are in agreement with the recent results reported by Du et al[42] that describe an ENU mouse mutant in *Tmprss6* with a similar phenotype. Lack of matriptase-2 causes an iron deficiency anemia and a hair loss phenotype, characterized by hepcidin up-regulation and the blockade of intestinal iron export into plasma. On the basis of the results presented herein, we propose that matriptase-2–mediated functions constitute a novel step in hepcidin regulation. The recent finding that mutations in the human *TMPRSS6* gene cause iron-refractory iron deficiency anemia (IRIDA)[43] turns *Tmprss6*^{−/−} mice into a useful genetic model for the analysis of molecular mechanisms that underlie human hematologic disorders whose molecular basis is yet unclear.

Authorship

Contribution: G.V. and C.L-O. designed the experimental work; A.R.F., F.M.L., A.M.P., C.G., F.R., A.A., T.B., and G.V. performed research; A.R.F., F.M.L., A.M.P., C.G., F.R., A.A., T.B., R.C., G.V., and C.L-O. analyzed data; and G.V., A.R.F. and C.L-O. wrote the paper.

Conflict-of-interest disclosure: The authors declare no competing financial interests.

Correspondence: Carlos Lopez-Otin, Departamento de Bioquímica y Biología Molecular, Facultad de Medicina, Universidad de Oviedo, 33006 Oviedo, Spain; e-mail: clo@uniovi.es.

References

1. Werb Z. ECM and cell surface proteolysis: regulating cellular ecology. Cell. 1997;91:439-442.

2. Netzel-Arnett S, Hooper JD, Szabo R, et al. Membrane anchored serine proteases: a rapidly expanding group of cell surface proteolytic enzymes with potential roles in cancer. Cancer Metastasis Rev. 2003;22:237-258.

3. Szabo R, Bugge TH. Type II transmembrane serine proteases in development and disease. Int J Biochem Cell Biol. 2008;40:1297-1316.

4. Kitamoto Y, Yuan X, Wu Q, McCourt DW, Sadler JE. Enterokinase, the initiator of intestinal digestion, is a mosaic protease composed of a distinctive assortment of domains. Proc Natl Acad Sci U S A. 1994;91:7588-7592.

5. Leytus SP, Loeb KR, Hagen FS, Kurachi K, Davie EW. A novel trypsin-like serine protease (hepsin) with a putative transmembrane domain expressed by human liver and hepatoma cells. Biochemistry. 1988;27:1067-1074.

6. Dhanasekaran SM, Barrette TR, Ghosh D, et al. Delineation of prognostic biomarkers in prostate cancer. Nature. 2001;412:822-826.

7. Bugge TH, List K, Szabo R. Matriptase-dependent cell surface proteolysis in epithelial development and pathogenesis. Front Biosci. 2007;12:5060-5070.

8. List K, Szabo R, Molinolo A, et al. Deregulated matriptase causes ras-independent multistage carcinogenesis and promotes ras-mediated malignant transformation. Genes Dev. 2005;19:1934-1950.

9. List K, Haudenschild CC, Szabo R, et al. Matriptase/MT-SP1 is required for postnatal survival, epidermal barrier function, hair follicle development, and thymic homeostasis. Oncogene. 2002;21:3765-3779.

10. Chan JC, Knudson O, Wu F, Morser J, Dole WP, Wu Q. Hypertension in mice lacking the proatrial natriuretic peptide convertase corin. Proc Natl Acad Sci U S A. 2005;102:785-790.

11. Lin B, Ferguson C, White JT, et al. Prostate-localized and androgen-regulated expression of the membrane-bound serine protease TMPRSS2. Cancer Res. 1999;59:4180-4184.

12. Wallrapp C, Hahnel S, Muller-Pillasch F, et al. A novel transmembrane serine protease (TMPRSS3) overexpressed in pancreatic cancer. Cancer Res. 2000;60:2602-2606.

13. Yamaguchi N, Okui A, Yamada T, Nakazato H, Mitsui S. Spinesin/TMPRSS5, a novel transmembrane serine protease, cloned from human spinal cord. J Biol Chem. 2002;277:6806-6812.

14. Kim DR, Sharmin S, Inoue M, Kido H. Cloning and expression of novel mosaic serine proteases with and without a transmembrane domain from human lung. Biochim Biophys Acta. 2001;1518:204-209.

15. Szabo R, Netzel-Arnett S, Hobson JP, Antalis TM, Bugge TH. Matriptase-3 is a novel phylogenetically preserved membrane-anchored serine protease with broad serpin reactivity. Biochem J. 2005;390:231-242.

16. Cal S, Quesada V, Garabaya C, Lopez-Otin C.

Polyserase-I, a human polyprotease with the ability to generate independent serine protease domains from a single translation product. Proc Natl Acad Sci U S A. 2003;100:9185-9190.

17. Yamaoka K, Masuda K, Ogawa H, Takagi K, Umemoto N, Yasuoka S. Cloning and characterization of the cDNA for human airway trypsin-like protease. J Biol Chem. 1998;273:11895-11901.

18. Hobson JP, Netzel-Arnett S, Szabo R, et al. Mouse DESC1 is located within a cluster of seven DESC1-like genes and encodes a type II transmembrane serine protease that forms serpin inhibitory complexes. J Biol Chem. 2004;279: 46981-46994.

19. Velasco G, Cal S, Quesada V, Sanchez LM, Lopez-Otin C. Matriptase-2, a membrane-bound mosaic serine proteinase predominantly expressed in human liver and showing degrading activity against extracellular matrix proteins. J Biol Chem. 2002;277:37637-37646.

20. Ramsay AJ, Reid JC, Velasco G, Quigley JP, Hooper JD. The type II transmembrane serine protease matriptase-2–identification, structural features, enzymology, expression pattern and potential roles. Front Biosci. 2008;13:569-579.

21. Parr C, Sanders AJ, Davies G, et al. Matriptase-2 inhibits breast tumor growth and invasion and correlates with favorable prognosis for breast cancer patients. Clin Cancer Res. 2007;13:3568-3576.

22. Lopez-Otin C, Overall CM. Protease degradomics: a new challenge for proteomics. Nat Rev Mol Cell Biol. 2002;3:509-519.

23. Lopez-Otin C, Matrisian LM. Emerging roles of proteases in tumour suppression. Nat Rev Cancer. 2007;7:800-808.

24. Hooper JD, Campagnolo L, Goodarzi G, Truong TN, Stuhlmann H, Quigley JP. Mouse matriptase-2: identification, characterization and comparative mRNA expression analysis with mouse hepsin in adult and embryonic tissues. Biochem J. 2003;373:689-702.

25. National Center for Biotechnology Information. Gene Expression Omnibus Database. http://www.ncbi.nlm.nih.gov/geo. Accessed June, 20, 2008.

26. Zheng B, Mills AA, Bradley A. A system for rapid generation of coat color-tagged knockouts and defined chromosomal rearrangements in mice. Nucleic Acids Res. 1999;27:2354-2360.

27. De Domenico I, McVey Ward D, Kaplan J. Regulation of iron acquisition and storage: consequences for iron-linked disorders. Nat Rev Mol Cell Biol. 2008;9:72-81.

28. Andrews NC. Iron homeostasis: insights from genetics and animal models. Nat Rev Genet. 2000; 1:208-217.

29. Schmidt PJ, Toran PT, Giannetti AM, Bjorkman PJ, Andrews NC. The transferrin receptor modulates hfe-dependent regulation of hepcidin expression. Cell Metab. 2008;7:205-214.

30. Park CH, Valore EV, Waring AJ, Ganz T. Hepcidin, a urinary antimicrobial peptide synthesized in the liver. J Biol Chem. 2001;276:7806-7810.

31. Nicolas G, Bennoun M, Devaux I, et al. Lack of hepcidin gene expression and severe tissue iron overload in upstream stimulatory factor 2 (USF2) knockout mice. Proc Natl Acad Sci U S A. 2001; 98:8780-8785.

32. Weinstein DA, Roy CN, Fleming MD, Loda MF, Wolfsdorf JI, Andrews NC. Inappropriate expression of hepcidin is associated with iron refractory anemia: implications for the anemia of chronic disease. Blood. 2002;100:3776-3781.

33. Nicolas G, Bennoun M, Porteu A, et al. Severe iron deficiency anemia in transgenic mice expressing liver hepcidin. Proc Natl Acad Sci U S A. 2002;99:4596-4601.

34. Nemeth E, Tuttle MS, Powelson J, et al. Hepcidin regulates cellular iron efflux by binding to ferroportin and inducing its internalization. Science. 2004;306:2090-2093.

35. Donovan A, Lima CA, Pinkus JL, et al. The iron exporter ferroportin/Slc40a1 is essential for iron homeostasis. Cell Metab. 2005;1:191-200.

36. Nicolas G, Chauvet C, Viatte L, et al. The gene encoding the iron regulatory peptide hepcidin is regulated by anemia, hypoxia, and inflammation. J Clin Invest. 2002;110:1037-1044.

37. Tanno T, Bhanu NV, Oneal PA, et al. High levels of GDF15 in thalassemia suppress expression of the iron regulatory protein hepcidin. Nat Med. 2007;13:1096-1101.

38. Babitt JL, Huang FW, Wrighting DM, et al. Bone morphogenetic protein signaling by hemojuvelin regulates hepcidin expression. Nat Genet. 2006; 38:531-539.

39. Lin L, Goldberg YP, Ganz T. Competitive regulation of hepcidin mRNA by soluble and cell-associated hemojuvelin. Blood. 2005;106:2884-2889.

40. Silvestri L, Pagani A, Camaschella C. Furin-mediated release of soluble hemojuvelin: a new link between hypoxia and iron homeostasis. Blood. 2008;111:924-931.

41. Singhatanadgit W, Salih V, Olsen I. Shedding of a soluble form of BMP receptor-IB controls bone cell responses to BMP. Bone. 2006;39:1008-1017.

42. Du X, She E, Gelbart T, et al. The serine protease TMPRSS6 is required to sense iron deficiency. Science. 2008;320:1088-1092.

43. Finberg KE, Heeney MM, Campagna DR, et al. Mutations in TMPRSS6 cause iron-refractory iron deficiency anemia (IRIDA). Nat Genet. 2008;40: 569-571.